CLINICAL RESEARCH

Plasma Ceramides as Prognostic Biomarkers and Their Arterial and Myocardial Tissue Correlates in Acute Myocardial Infarction

Leonardo P. de Carvalho, MD, PHD,[a,b,c,d] Sock Hwee Tan, PHD,[b,c] Ghim-Siong Ow, BSc,[e] Zhiqun Tang, PHD,[e,f]
Jianhong Ching, PHD,[g] Jean-Paul Kovalik, MD, PHD,[g] Sock Cheng Poh, BSc,[b] Chee-Tang Chin, MBBS,[g,h]
A. Mark Richards, MD, PHD,[b,i] Eliana C. Martinez, MD, PHD,[j] Richard W. Troughton, MD, PHD,[i]
Alan Yean-Yip Fong, MBBS,[k,l] Bryan P. Yan, MBBS,[m] Aruni Seneviratna, MBBS, MPH,[b] Vitaly Sorokin, MD, PHD,[b,c]
Scott A. Summers, PHD,[n] Vladimir A. Kuznetsov, PHD, ScID,[e,o] Mark Y. Chan, MBBS, PHD[b,c]

JACC: BASIC TO TRANSLATIONAL SCIENCE CME/MOC

This article has been selected as the month's *JACC: Basic to Translational Science* CME/MOC activity, available online at http://www.acc.org/jacc-journals-cme by selecting the *JACC* Journals CME/MOC tab.

Accreditation and Designation Statement

The American College of Cardiology Foundation (ACCF) is accredited by the Accreditation Council for Continuing Medical Education (ACCME) to provide continuing medical education for physicians.

The ACCF designates this journal-based CME/MOC activity for a maximum of 1 *AMA PRA Category 1 Credit(s)*. Physicians should only claim credit commensurate with the extent of their participation in the activity.

Method of Participation and Receipt of CME/MOC Certificate

To obtain credit for *JACC: Basic to Translational Science* CME/MOC, you must:
1. Be an ACC member or *JACC: Basic to Translational Science* subscriber.
2. Carefully read the CME/MOC-designated article available online and in this issue of the journal.
3. Answer the post-test questions. At least 2 out of the 3 questions provided must be answered correctly to obtain CME/MOC credit.
4. Complete a brief evaluation.
5. Claim your CME/MOC credit and receive your certificate electronically by following the instructions given at the conclusion of the activity.

CME/MOC Objective for This Article: Upon completion of this activity, the learner should be able to: 1) examine the role of the ceramide signature to predict outcomes, including 12-month death, myocardial infarction, and stroke, in acute myocardial infarction patients; 2) assess the mechanism by which ceramide levels are increased in ischemic myocardium; and

3) explore the acute management of myocardial infarction and how other commonly used biomarkers are utilized to predict major adverse cardiovascular events.

CME/MOC Editor Disclosure: CME/MOC Editor L. Kristin Newby, MD, is supported by research grants from Amylin, Bristol-Myers Squibb Company, GlaxoSmithKline, Sanofi-Aventis, Verily Life Sciences (formerly Google Life Sciences), the MURDOCK Study, NIH, and PCORI; receives consultant fees/honoraria from BioKier, DemeRx, MedScape/TheHeart.org, Metanomics, Philips Healthcare, Roche Diagnostics, CMAC Health Education & Research Institute; serves as an Officer, Director, Trustee, or other Fiduciary Role for AstraZeneca HealthCare Foundation and the Society of Chest Pain Centers (now part of ACC); and serves in another role for the American Heart Association and is the Deputy Editor of *JACC: Basic to Translational Science*.

Medium of Participation: Online (article and quiz).
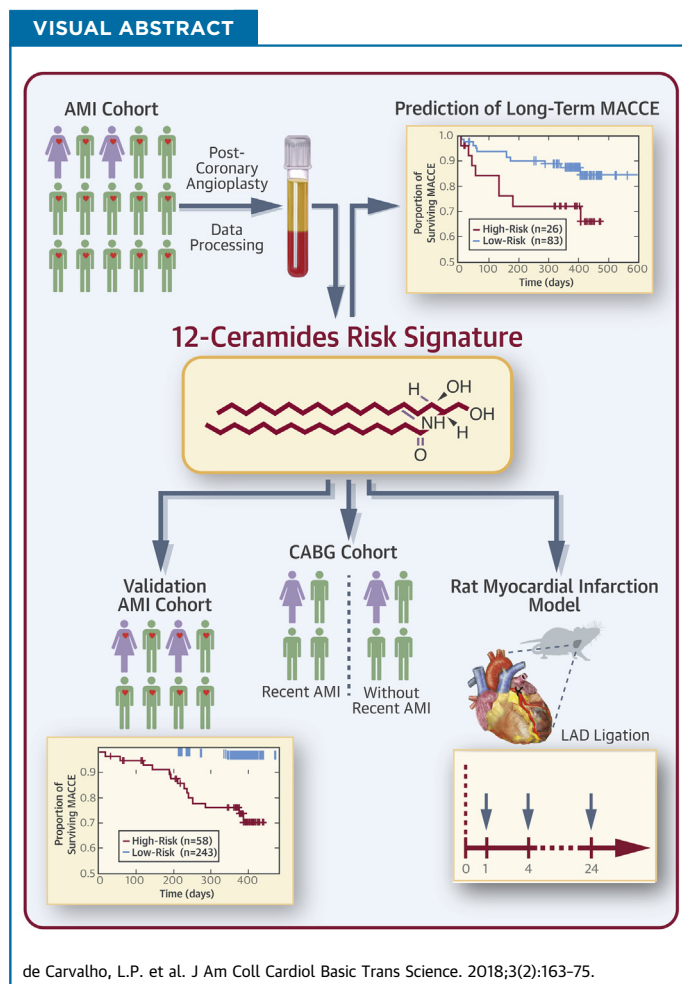
CME/MOC Term of Approval

Issue Date: April 2018
Expiration Date: March 31, 2019

From the [a]Federal University of Sao Paulo State, Sao Paulo, Brazil; [b]National University Heart Center, Singapore, Singapore; [c]Cardiovascular Research Institute, Yong Loo Lin School of Medicine, National University of Singapore, Singapore; [d]Albert Einstein Hospital, São Paulo, Brazil; [e]Bioinformatics Institute, A*STAR, Singapore; [f]Institute of Molecular and Cell Biology, A*STAR, Singapore; [g]Program in Cardiovascular and Metabolic Disorders, Duke-National University of Singapore Graduate Medical School, Singapore; [h]National Heart Centre Singapore, Singapore; [i]Christchurch Heart Institute, University of Otago Christchurch, Christchurch Hospital, Christchurch, New Zealand; [j]Miller School of Medicine, University of Miami, Miami, Florida; [k]Clinical Research Centre, Sarawak General Hospital, Kuching, Malaysia; [l]Department of Cardiology, Sarawak General Hospital, Kuching, Malaysia; [m]Department of Medicine & Therapeutics, The Chinese University of Hong Kong, Hong Kong, China;

Plasma Ceramides as Prognostic Biomarkers and Their Arterial and Myocardial Tissue Correlates in Acute Myocardial Infarction

Leonardo P. de Carvalho, MD, PhD,[a,b,c,d] Sock Hwee Tan, PhD,[b,c] Ghim-Siong Ow, BSc,[e] Zhiqun Tang, PhD,[e,f]
Jianhong Ching, PhD,[g] Jean-Paul Kovalik, MD, PhD,[g] Sock Cheng Poh, BSc,[b] Chee-Tang Chin, MBBS,[g,h]
A. Mark Richards, MD, PhD,[b,i] Eliana C. Martinez, MD, PhD,[j] Richard W. Troughton, MD, PhD,[i]
Alan Yean-Yip Fong, MBBS,[k,l] Bryan P. Yan, MBBS,[m] Aruni Seneviratna, MBBS, MPH,[b] Vitaly Sorokin, MD, PhD,[b,c]
Scott A. Summers, PhD,[n] Vladimir A. Kuznetsov, PhD, ScID,[e,o] Mark Y. Chan, MBBS, PhD[b,c]

VISUAL ABSTRACT

de Carvalho, L.P. et al. J Am Coll Cardiol Basic Trans Science. 2018;3(2):163–75.

HIGHLIGHTS

- **Targeted profiling of ceramides identified a 12-ceramide plasma signature that predicted 12-month cardiovascular death, MI, and stroke in 2 prospective cohorts of AMI patients.**

- **Among coronary artery bypass grafting patients, plasma ceramides were higher in those with recent AMI compared with those without recent acute MI.**

- **Analysis of rat ischemic myocardium revealed a consistent increase in ceramide levels and overexpression of 3 enzymes in ceramide biosynthesis.**

SUMMARY

We identified a plasma signature of 11 C14 to C26 ceramides and 1 C16 dihydroceramide predictive of major adverse cardiovascular events in patients with acute myocardial infarction (AMI). Among patients undergoing coronary artery bypass surgery, those with recent AMI, compared with those without recent AMI, showed a significant increase in 5 of the signature's 12 ceramides in plasma but not simultaneously-biopsied aortic tissue. In contrast, a rat AMI model, compared with sham control, showed a significant increase in myocardial concentrations of all 12 ceramides and up-regulation of 3 ceramide-producing enzymes, suggesting ischemic myocardium as a possible source of this ceramide signature. (J Am Coll Cardiol Basic Trans Science 2018;3:163–75) © 2018 The Authors. Published by Elsevier on behalf of the American College of Cardiology Foundation. This is an open access article under the CC BY-NC-ND license (http://creativecommons.org/licenses/by-nc-nd/4.0/).

A s many as 10% of the patients hospitalized for acute myocardial infarction (AMI) will have another episode of AMI within 12 months of the index hospitalization (1). Apart from cholesterol, recent studies have highlighted the physiological role of other lipid classes in atherosclerosis and AMI, including ceramides, sphingomyelin, phosphatidylcholines, and cholesterol esters (2-4).

Of these lipids, ceramides are among the most bioactive membrane lipids regulating signal transduction pathways that lead to cell survival or death (5). Ceramides accumulate in coronary atheromatous plaque (3), and their glycosylated forms, glucosylceramides and lactosylceramides, are more abundant in regions of arterial tissue with visible plaque development (2). Myocardium can produce ceramides in response to ischemia and reperfusion, leading to an increase of ceramides that activate mitochondrial autophagy and apoptosis (6,7). As plasma ceramides are now readily quantifiable, it has become possible to examine the relationship between ceramides and cardiovascular death in stable and unstable coronary artery disease (CAD) cohorts (4,8,9). Although associations between ceramides and cardiovascular death have been observed, the association between plasma ceramides and incident MI has only recently emerged (4,10).

To evaluate the prognostic role and tissue origin of plasma ceramides in AMI, we studied the association of ceramides with cardiovascular death, recurrent MI, and stroke to construct a prognostic ceramide signature. The prognostic utility of the ceramide signature was validated in an independent AMI cohort. We then further characterized the arterial and myocardial profiles of the signature's individual ceramides in human aortic biopsy samples and a rodent AMI model, respectively.

METHODS

STUDY DESIGN. Discovery cohort. Plasma samples were obtained from patients undergoing invasive management for AMI at 2 tertiary hospitals in Singapore between 2011 and 2013 (Supplemental Figure 1). Blood samples were collected pre-angiography (day 1) and within 24 h post-angiography (day 2). We included 337 patients with AMI who were diagnosed following the criteria from the Third Universal Definition of Myocardial Infarction (11), as ascertained by the managing physician. All patients underwent coronary angiography within 7 days of symptom onset and within 3 days of hospitalization. Exclusion criteria included low hemoglobin concentration (<8 g/l for men and <7 g/l for women), unwillingness to give consent, or absence of obstructive CAD, defined as any stenosis ≥70% or left main stenosis ≥50% (12). All patients were contacted by phone up to 24 months after the index hospitalization to ascertain the incidence of major adverse cardiac and cerebrovascular events (MACCE).

Validation cohort. Plasma samples were obtained from an independent cohort of 119 patients undergoing invasive management for clinically diagnosed AMI and who had obstructive CAD on coronary angiography at the Christchurch Hospital (Christchurch, New Zealand) between 2013 and 2014. Blood samples were collected at 24 h post-angiography (day 2), and all patients received follow-up phone calls up to 24 months after the index hospitalization (Supplemental Figure 1).

Animal study. All animal experiments were approved by the Institutional Animal Care and Use Committee of the National University of Singapore and were performed in accordance with the established guiding principles for animal research

(Supplemental Appendix). Briefly, male Wistar rats (250 to 300 g) underwent permanent ligation of the left anterior descending artery, sham thoracotomy, or anesthesia without surgery (AMI/sham/healthy groups). The combination of isoflurane for anesthesia, pentobarbital for euthanasia, and organ harvesting during anesthesia rather than post-euthanasia has been shown to minimally perturb the rodent metabolome (13).

Human arterial tissue and plasma. A total of 70 patients undergoing elective coronary artery bypass grafting (CABG) with (n = 35) or without (n = 35) who incurred AMI within 2 weeks prior to surgery were recruited. Standard full normothermic cardiopulmonary bypass (37°C) and cold (4°C) anterograde cardioplegia were performed. Proximal anastomoses were created by punch biopsies of the aorta during CABG; the punch biopsy tissues were snap-frozen immediately and stored at −196°C until used. Simultaneous peripheral blood samples were also collected, and plasma was stored at −80°C.

LIPID EXTRACTION. Please refer to the Supplemental Appendix for details regarding lipid extraction.

MEASUREMENT OF LIPID SPECIES. HPLC-grade acetonitrile and ammonium acetate were purchased from Sigma-Aldrich (St. Louis, Missouri). A total of 68 ceramide species (Supplemental Table 1) were quantified by hydrophilic interaction LC (HILIC) MS/MS at Duke-National University of Singapore Graduate Medical School (Singapore). Extracted lipids were separated on an HILIC column (Thermo Fisher Scientific, Waltham, Massachusetts) (100 × 2.1 mm; particle size 2.6 μm) using an Agilent 1260 LC system coupled to an Agilent 6430 triple quadrupole mass spectrometer (Agilent Technologies, Santa Clara, California). Briefly, the HILIC column was equilibrated with 100% mobile phase A (acetonitrile/water [95:5] with 10 mmol/l ammonium acetate, pH 8.0), increasing to 20% mobile phase B (acetonitrile/water [50:50] with 10 mmol/l ammonium acetate, pH 8.0) in 5 min, then held for 5 min. The column was finally re-equilibrated with 100% mobile phase A for 5 min. Peak detection was performed using the Quantitative Analysis for QqQ (version B.06.00, Agilent). Chromatography peaks were autointegrated and manually curated. Lipid concentrations were estimated by comparing the peak area of each species to the peak area of the corresponding internal standard. Blank runs (mobile phase B) were included every 5 samples to assess the extent of carryover.

RNA ISOLATION AND REAL-TIME PCR. Please refer to the Supplemental Appendix for details regarding RNA isolation and real-time PCR.

STATISTICAL ANALYSIS. Baseline characteristics of continuous and categorical variables were presented as mean ± SD and percentage, respectively. Continuous variable sets were compared using the Student t test and Mann-Whitney U test for parametric and nonparametric tests, respectively, whereas categorical variable sets were compared using the chi-square and Fisher exact tests. Dependent variable comparison was carried out using the paired Student t test and Wilcoxon matched pairs test. Pearson and Kendall's tau correlation coefficient values were calculated to understand correlation patterns between different variables.

Rat myocardial and human aortic ceramide intensities were normalized to tissues' wet weights (Supplemental Appendix, Supplemental Figure 2). The fold-changes of paired human aortic tissue and plasma were calculated via the ratio of their median intensities. The statistical significance of the differential intensity values for the plasma and tissue samples was assessed via the nonparametric Mann-Whitney U test. For the comparison of rat myocardial and plasma samples among healthy, sham, and MI groups, we applied 2-way analysis of variance with ceramide concentration as one factor and healthy/sham/MI group as the other factor. The p value for interaction between these 2 factors was 0.01.

The prognostic association of individual ceramide species with MACCE and time of the event was modelled using Cox Proportional Hazards regression. Clinical risk factors, including components of the GRACE (Global Registry of Acute Coronary Events) risk score (14), were adjusted in the Cox regression model. Time-to-event survival functions for each ceramide were estimated and visualized via the Kaplan-Meier survival curve analyses, with low- and high- risk groups compared by the log-rank test.

We then used deep-learning predictor selection and risk stratification methods (data-driven grouping [DDg] and statistically-weighted voting grouping [SWVg], respectively) (Supplemental Figure 3). This model, which we had previously developed and validated (15-20), is described in the Supplemental Appendix. Briefly, at the first step of the method, we apply the DDg method to identify cut-off values (intensities) of individual prognostic variables (i.e., ceramides) that optimally separate patients into low- and high-risk MACCE groups, In the second step, the SWVg method utilizes the 1D-DDg–defined ceramide risk categories for each patient and combines ceramides in a stepwise multivariable fashion to produce a synergistic multiceramide signature. To define a robust prognostic signature, we only included component ceramides that were statistically

significant in all 3 models: Cox regression, DDg, and SWVg. A 2-sided alpha of 0.05 was considered statistically significant, and the false discovery rate was set at 0.1. Because patients either do or do not have events and because of sample size limitations, multiple risk categories were avoided. Thus, 2 prognostically distinct risk categories, low-risk and high-risk, were considered. At this consideration, SVWg optimization procedure (17) defined the 12 ceramides that collectively provided most confidence discrimination of the low- and high-risk patients. Finally, a linear regression model was used for the quantitative analysis of the association between datasets and testing their scalability (Supplemental Appendix, Supplemental Figure 4). Regular statistical analyses were performed on GraphPad Prism version 5 (GraphPad, San Diego, California), Statistica 7.1 (Tulsa, Oklahoma), ComBat (21), and SurvExpress (22).

STUDY APPROVAL. The study was conducted according to the Helsinki Declaration, and all institutions' human ethics review boards approved the study protocol. Animal experiments were approved by the institutional animal care and use committee of the National University of Singapore.

RESULTS

THE CLINICAL CHARACTERISTICS AND BIOCHEMICAL PROFILES OF THE AMI PATIENTS. The clinical characteristics and biochemical profiles of the AMI patients are shown in Table 1. Compared with the validation cohort, patients in the discovery cohort were significantly younger; more likely to be men and smokers; and more likely to have diabetes mellitus, dyslipidemia, and a lower body mass index (p < 0.05). Mean levels of triglycerides and low-density lipoprotein cholesterol were not significantly different between the 2 cohorts. Mean high-density lipoprotein cholesterol showed a nonsignificant trend toward lower levels in the Singapore discovery cohort.

CORRELATIONS AND DIFFERENCES OF THE PLASMA CERAMIDES MEASURED PRE-ANGIOGRAPHY AND WITHIN 24 H POST-ANGIOGRAPHY. Of the 68 ceramides measured, 14 ceramides and 6 dihydroceramides (DHCer) were reproducibly detected in plasma. The concentrations of 8 of 14 ceramides (Cer d18:1/14:0, d18:1/18:1[9Z], d18:1/20:0, d18:1/22:0, d18:1/23:0, d18:1/24:0, d18:1/25:0, and d18:1/26:0) and all 6 DHCer (DHCer d18:0/16:0, d18:0/18:0, d18:0/20:0, d18:0/22:0, d18:0/24:0, and d18:0/24:1[15Z]) were significantly lower at day 2 compared with day 1 (Supplemental Table 2).

During a median follow-up of 12 months, 26 of the 327 discovery cohort patients and 25 of the 119

TABLE 1	Baseline Characteristics of Discovery and Validation Cohorts		
	Discovery Cohort (Singapore) (n = 337)	**Validation Cohort (New Zealand) (n = 119)**	**p Value**
Age, yrs	57.5 ± 10.5	66.2 ± 10.7	1.69×10^{-12}
Female	35 (10.4)	33 (27.7)	1.00×10^{-5}
Body mass index, kg/m²	25.7 ± 3.72	28.7 ± 5.56	5.35×10^{-8}
Diabetes	131 (38.9)	23 (19.3)	1.68×10^{-4}
Hypertension	232 (68.8)	68 (57.1)	0.0278
Dyslipidemia	233 (69.1)	64 (53.8)	0.00361
Prior AMI	88 (26.1)	40 (33.6)	0.148
Smoking	140 (41.6)	16 (13.4)	6.02×10^{-8}
Race			
Caucasian	14 (4.2)	117 (97.4)	NA
Chinese	197 (58.5)	1 (0.84)	NA
Indian	41 (12.2)	1 (0.84)	NA
Malay	84 (24.9)	1 (0.84)	NA
NST-ACS	245 (72.7)	78 (65.5)	0.174
GRACE score	96.9 ± 24.9	114 ± 29.5	1.49×10^{-8}
Hemoglobin A1c, %	7.29 ± 2.12	6.36 ± 1.22	0.064
Total cholesterol, mmol/l	4.98 ± 1.2	5.03 ± 1.5	0.751
TG, mmol/dl	1.83 ± 1.17	1.78 ± 1.01	0.969
HDL, mmol/dl	1.07 ± 0.275	1.34 ± 1.01	0.067
LDL, mmol/dl	3.16 ± 1.07	3.09 ± 1.27	0.272
Revascularization	245 (72.7)	89 (74.8)	0.928

Values are mean ± SD or n (%). For comparison between the discovery and validation cohort, Mann-Whitney *U* tests were used for continuous variables and chi-square tests were used for categorical variables. p values for Mann-Whitney *U* tests are 2-sided. p < 0.05 was considered statistically significant.

AMI = acute myocardial infarction; GRACE = Global Registry of Acute Coronary Events; HDL = high-density lipoprotein; LDL = low-density lipoprotein; NA = not applicable; NST-ACS = non–ST-segment elevation acute coronary syndrome(s); TG = triglycerides.

validation cohort patients had their first MACCE event, respectively. Cox proportional hazards regression analysis performed for each ceramide, with adjustment for the GRACE score, indicated 11 and 14 of the quantifiable ceramides (at days 1 and 2, respectively) yielded significant hazard ratios for MACCE in the discovery cohort (Table 2).

Table 2 shows that 10 ceramides are survival significant at both days 1 and 2 (p ≤ 0.05); additionally, 1 ceramide was significant at day 1, and 4 ceramides at day 2. Kendall's tau correlation coefficient between −log₂ (p value) at days 1 and 2 was 0.507 (p = 0.001). The individual ceramide measurements at day 2 had smaller p values than at day 1.

Thus, we conclude that high-risk patients have an overexpression of the selected plasma ceramides on days 1 and 2; however, day 2 ceramides more accurately identified patients who were at high-risk of MACCE.

IDENTIFICATION OF THE MULTICERAMIDE PROGNOSTIC SIGNATURE. Supplemental Figure 3 shows the workflow of the discovery and validation analyses. Supplemental Table 3 shows that 20 ceramides measured at day 2 were significant for MACCE-free survival (false discovery rate <0.05). Notably, for 18

TABLE 2 Association of Day 1 and 2 Ceramide Species With 12-Month MACCE				
	Pre-Angiography (Day 1)		Post-Angiography (Day 2)	
	Hazard Ratio (95% CI)	p Value	Hazard Ratio (95% CI)	p Value
Cer(d18:1/14:0)	1.703 (0.40–7.27)	0.4723	2.764 (0.72–10.67)	0.1400
Cer(d18:1/16:0)	1.031 (1.01–1.05)	0.0048	1.030 (1.01–1.05)	0.0036
Cer(d18:1/18:0)	1.049 (0.99–1.12)	0.1314	1.057 (1.00–1.12)	0.0589
Cer(d18:1/18:1[9Z])	4.623 (1.02–20.96)	0.0471	3.966 (0.75–21.09)	0.1060
Cer(d18:1/20:0)	1.089 (0.98–1.21)	0.1002	1.135 (1.04–1.24)	0.0045
Cer(d18:1/20:4)	2.792 (0.64–12.17)	0.1716	4.715 (0.68–32.64)	0.1161
Cer(d18:1/22:0)	1.013 (1.00–1.03)	0.0497	1.022 (1.00–1.04)	0.0117
Cer(d18:1/22:1)	1.478 (0.91–2.40)	0.1133	1.744 (1.31–2.33)	0.0002
Cer(d18:1/23:0)	1.020 (1.00–1.04)	0.0541	1.030 (1.00–1.06)	0.0201
Cer(d18:1/24:0)	1.004 (1.00–1.01)	0.0754	1.007 (1.00–1.01)	0.0093
Cer(d18:1/24:1[15Z])	1.015 (1.01–1.02)	0.0011	1.025 (1.01–1.04)	0.0002
Cer(d18:1/25:0)	1.122 (1.03–1.23)	0.0118	1.249 (1.11–1.40)	0.0001
Cer(d18:1/26:0)	1.773 (0.90–3.49)	0.0968	1.968 (0.99–3.90)	0.0522
Cer(d18:1/26:1[17Z])	3.250 (1.49–7.10)	0.0031	4.924 (2.10–11.55)	0.0002
DHCer(d18:0/16:0)	1.861 (1.19–2.92)	0.0068	2.363 (1.19–4.68)	0.0136
DHCer(d18:0/18:0)	1.588 (1.09–2.32)	0.0163	1.848 (1.25–2.73)	0.0020
DHCer(d18:0/20:0)	1.465 (1.12–1.91)	0.0048	1.315 (1.08–1.60)	0.0072
DHCer(d18:0/22:0)	1.124 (1.01–1.25)	0.0325	1.094 (1.00–1.20)	0.0623
DHCer(d18:0/24:0)	1.073 (0.98–1.17)	0.1091	1.080 (1.01–1.15)	0.0235
DHCer(d18:0/24:1[15Z])	1.097 (1.04–1.16)	0.0008	1.122 (1.06–1.19)	0.0001

There are 314 samples for day 1 and 309 samples for day 2. For each ceramide, Cox proportional hazards regression analysis was performed by using plasma ceramide as the independent variable and Global Registry of Acute Coronary Events Risk score as the confounding variable. The p value was calculated via Wald's test. $p < 0.05$ was considered statistically significant.

Cer = ceramide; CI = confidence interval; DHCer = dihydroceramide.

of the 20 ceramides selected in the discovery cohort, the 1D-DDg–defined cut-off values better stratified patients into low- and high-risk patient groups compared with the GRACE score. Supplemental Table 3 summarizes the univariate 1D-DDg and multivariate SWVg models used in the training cohort. As shown in **Figure 1A** (left), there was no significant difference between relatively low- and high-risk groups defined by GRACE score (at cut-off GRACE score = 141; p = 0.41) in the discovery cohort. The combination of 12 ceramides was highly predictive of 12-month MACCE (p = 3.17×10^{-10}) (**Figure 1B**, left). The survival curves after stratification into low- and high-risk groups using each of the top 12 ceramides are shown in Supplemental Figure 5.

VALIDATION OF THE 12-CERAMIDE PROGNOSTIC PLASMA SIGNATURE IN AN INDEPENDENT COHORT. The intensities of the plasma ceramides from both the discovery and validation cohort showed similar distributions that were scalable and well-calibrated (Supplemental Appendix, Supplemental Figure 4). When we dichotomized the patients in the validation cohort using the same cut-off intensities of the ceramides defined in the training cohort, we found that 11 of the 12 dichotomized ceramides were

directionally similar in the validation as in the training cohort. By the binomial test of the HO-hypothesis (random coincident events) this result was significant (p = 0.00468). Of the 12 ceramides, only Cer(d18:1/22:1) was statistically significant in the both cohorts (p < 0.05) (**Figure 1C,** Supplemental Figure 6). Several others trended toward statistical significance (for instance, Cer(d18:1/23:0), Cer(18:1/24:0), Cer(18:1/25:0), and Cer(d18:1/26:0) at p < 0.10) (see also Supplemental Figure 7). However, in validation cohort collectively, the 12-ceramide prognostic signature was statistically significant (p = 0.03875) (**Figure 1B**, right).

Due to the difference in sample size, with the available validation dataset being ~3× smaller than the discovery dataset, we expected that the results of implementation of the prognostic model parameters, defined by the 1D-DDg method at validation step, might be less stable and significant than in the training dataset (Supplemental Figures 6 and 7). The relatively small size of the validation cohort prohibited us from calculating calibration measures such as the Hosmer-Lemeshow chi-square test. However, we can infer from **Figures 1A to 1C** as to whether the GRACE score, 12-ceramide-defined score, and single ceramide predictors predict MACCE event rates uniformly in the discovery and validation cohorts (Supplemental Table 3). By comparing the MACCE-free survival rates of the GRACE score–defined low- and high-risk groups in the discovery and validation cohorts, we see that the GRACE score had the poorest reproducibility in predicting actual survival rates of both the low- and high-risk groups (**Figure 1A**). In contrast, low- and high-risk groups defined by an individual ceramide predictor yielded more similar MACCE-free survival rates in the discovery and validation cohorts, especially among the high-risk group (**Figure 1C**). The most reproducible MACCE-free survival rates were observed with the 12-ceramide risk signature (**Figure 1B**).

ARTERIAL AND PLASMA CERAMIDES IN AMI. We then sought to investigate changes in the 12-ceramide prognostic signature in human arterial tissue and plasma obtained concurrently after a recent AMI. Human ascending aortic punch biopsies and concomitant plasma samples were obtained during CABG in patients with (n = 35) and without (n = 35) AMI within 2 weeks prior to CABG (Supplemental Table 4). Compared with patients without recent AMI, those with recent AMI had higher levels of plasma Cer(d18:1/16:0), Cer(d18:1/18:0), Cer(d18:1/20:0), Cer(d18:1/24:1(15Z)), and DHCer(d18:0/16:0) (**Figure 2**), all of which were components of the 12-ceramide prognostic signature (**Table 3**). Aortic tissue samples from the same patients demonstrated

FIGURE 1 MACCE-Free Survival Plots of Patients Grouped by Multiceramide Species Signature to Predict Time to MACCE in the Discovery and Validation Cohorts
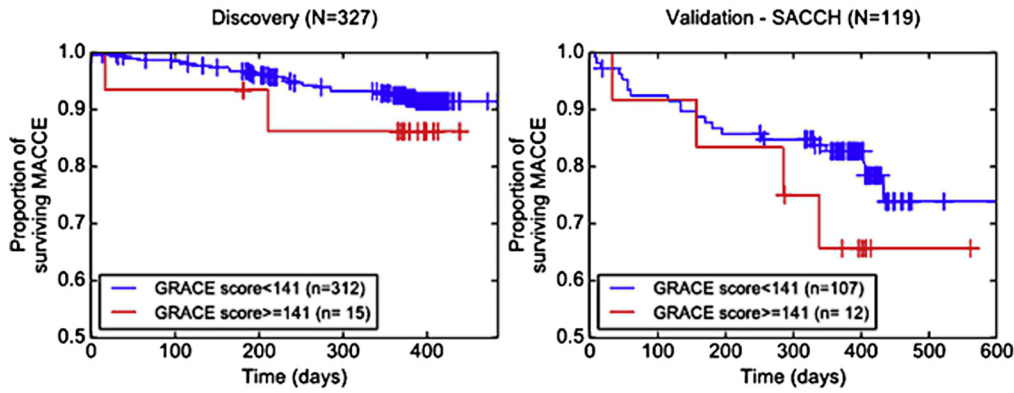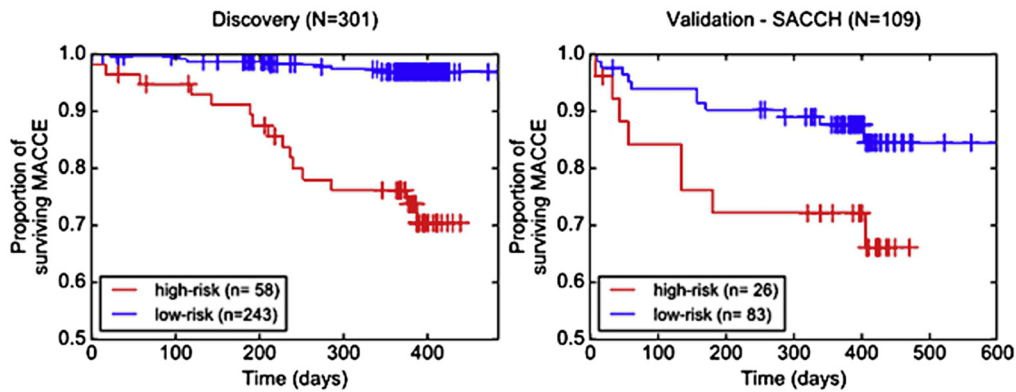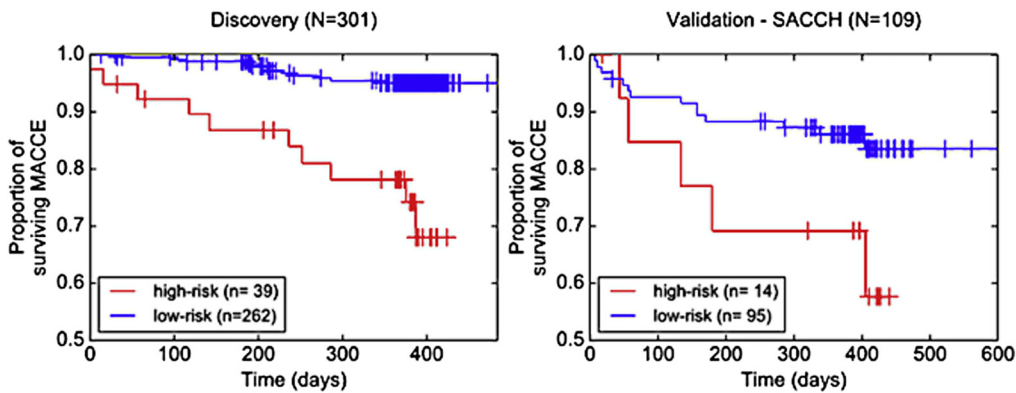
(A) Kaplan-Meier survival plots of patients stratified via GRACE (Global Registry of Acute Coronary Events) score cut-off value n $_{cut-off}$ = 141 in the discovery (Singapore) cohort and validation (Christchurch) cohort. (B) Kaplan-Meier survival plots of patients stratified via a 12-ceramide plasma signature in the discovery (Singapore-Asian) cohort and validation (Christchurch-Caucasian) (SACCH) cohort. (C) Kaplan-Meier survival plots of patients stratified via the plasma ceramide Cer(18.1/22.1) level in the discovery (Singapore-Asian) cohort and validation (Christchurch-Caucasian) cohort. **Red** indicates high-risk subgroup and **blue** indicates low-risk subgroup. MACCE = major adverse cardiac and cerebrovascular events.

FIGURE 2   Heat Map Showing the Fold Changes of Paired Aortic Tissue and Plasma Ceramide Levels in Patients With Versus Without Myocardial Infarction 2 Weeks Prior to Surgery

Patients with recent acute myocardial infarction (AMI) had higher levels of plasma and arterial ceramides than patients without recent AMI. **Red** represents an increase in levels, whereas **blue** represents a decrease in levels. **X** represents undetectable. *p < 0.05; **p < 0.01.
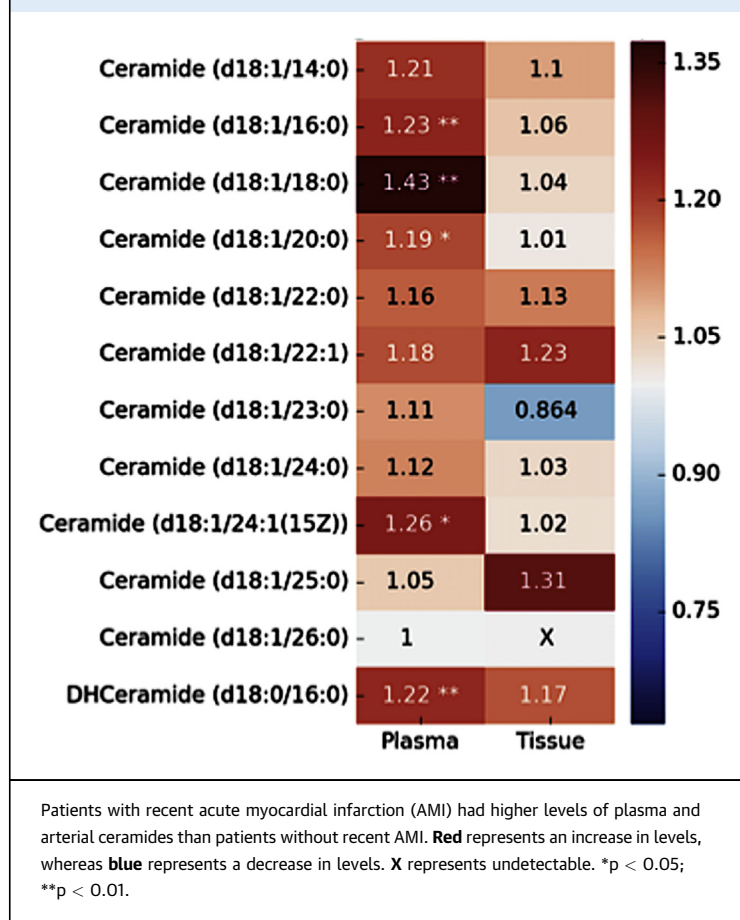
only a nonsignificant trend toward slightly higher ceramide levels in patient samples with versus those without recent AMI (**Figure 2**).

MYOCARDIAL CERAMIDES AND THEIR REGULATORY ENZYMES IN AMI. The use of an animal model of AMI allowed us to delineate the effect of acute ischemia and necrosis on plasma and myocardial ceramides and to study the related gene expression changes in enzymes involved in ceramide biosynthesis and degradation. The mortality at 1 h post-MI was 14.3% in our rat experiments. All deaths occurred during the first hour post–left anterior descending (LAD) ligation, whereas no mortality was observed in the sham groups. Following ligation of the LAD artery in rats (n = 6), we observed an increase in myocardial levels of individual ceramide species from the prognostic signature when compared with rats with or without sham surgery (n = 3) (**Figure 3A,** Supplemental Figures 8 and 9). Notably, the levels of 5 ceramides in myocardial tissue, Cer(d18:1/16:0), Cer(d18:1/18:0),

Cer(d18:1/20:0), Cer(d18:1/22:0), and Cer(d18:1/24:0), were significantly higher in the AMI group than in the sham control groups. In plasma samples obtained at the same timepoints via tail vein sampling, only Cer(d18.1/24.0) was significantly increased in the AMI group compared with sham and healthy animals, whereas the other plasma ceramides showed a numerical increase that was not statistically significant (**Figure 3B,** Supplemental Figures 10 and 11).

We then profiled gene expression changes of the enzymes involved in ceramide synthesis and degradation pathways to identify changes in myocardial enzyme gene expression 24 h after ligation of the LAD. Supplemental Figure 12 shows that there was an overexpression of serine palmitoyl transferase-2, ceramide synthase 6 (CerS6), and neutral sphingomyelinase (nSMase), and an underexpression of acid ceramidase in AMI versus sham control subjects. The serine palmitoyl transferase-2 gene encodes a long-chain base subunit of serine palmitoyl transferase (SPT), an enzyme that catalyzes the first step of the biosynthesis of sphingolipids. CerS6 encodes ceramide synthase 6, which is primarily involved in the de novo synthesis of C16:0 ceramides. nSMase encodes neutral sphingomyelinase, which metabolizes sphingomyelin into ceramides. Acid ceramidase is a lipid hydrolase that degrades ceramides into sphingosine and free fatty acids.

DISCUSSION

Ceramides, highly bioactive membrane lipids, have been implicated in atherosclerotic plaque progression (23-25) and ischemia-induced cardiomyocyte apoptosis (6,26). We identified a 12-ceramide plasma prognostic signature that predicted long-term MACCE in patients with AMI, of which Cer(d18:1/22:1), Cer(d18:1/24:1[15Z]), and DHCer(d18:0/16:0) were the strongest predictors of MACCE. Further profiling of the ceramide signature in patients undergoing CABG showed that plasma levels of 4 ceramides and 1 dihydroceramide were significantly higher in patients with versus without recent AMI. Aortic tissue from the same patients showed only a modest and nonsignificant numerical trend toward increased concentrations of these ceramide species when comparing patients with versus without recent AMI. Additionally, temporal profiling of myocardial ceramides and their regulatory enzymes in a rodent model of AMI demonstrated myocardial up-regulation of 3 ceramide production enzymes, SPT, CerS6, and nSMase, and down-regulation of 1 ceramide degradation enzyme, acid ceramidase, leading to a net increased production of all 12 ceramides in ischemic myocardium within 24 h of

TABLE 3 1-Dimensional Data-Driven Grouping and Statistically Weighted Voting Grouping Models Trained in the Discovery Cohort

		Univariate 1D-DDg Analysis				Multivariate SWVg Analysis				
	Intensity Cut-Off	Log-Rank p Value	Design*	Number of Low-Risk Subjects	Number of High-Risk Subjects	Number of Ceramides in the Signature†	Log-Rank p Value	Design*	Number of Low-Risk Subjects	Number of High-Risk Subjects
					Discovery Cohort					
1 Cer(d18:1/22:1)	2.27	5.368×10^{-7}	2	262	39	1	—	—	—	—
2 Cer(d18:1/24:1(15Z))	78.27	7.610×10^{-7}	2	262	39	2	—	—	—	—
3 DHCer(d18:0/16:0)	1.22	6.200×10^{-6}	2	244	57	3	1.210×10^{-8}	2	250	51
4 Cer(d18:1/20:0)	8.07	2.772×10^{-5}	2	203	98	4	3.219×10^{-9}	2	258	43
5 Cer(d18:1/25:0)	9.62	4.170×10^{-5}	2	261	40	5	5.923×10^{-10}	2	248	53
6 Cer(d18:1/16:0)	26.09	1.114×10^{-4}	2	160	141	6	3.164×10^{-10}	2	249	52
7 Cer(d18:1/18:0)	10.28	1.898×10^{-4}	2	191	110	7	3.164×10^{-10}	2	249	52
8 Cer(d18:1/26:0)	1.13	5.284×10^{-4}	2	244	57	8	3.173×10^{-10}	2	243	58
9 Cer(d18:1/22:0)	25.38	4.337×10^{-3}	2	75	226	9	3.173×10^{-10}	2	243	58
10 Cer(d18:1/24:0)	181.08	7.459×10^{-3}	2	267	34	10	6.094×10^{-10}	2	242	59
11 Cer(d18:1/14:0)	0.36	1.240×10^{-2}	2	83	218	11	1.604×10^{-10}	2	244	57
12 Cer(d18:1/23:0)	42.39	1.488×10^{-2}	2	265	36	12	3.173×10^{-10}	2	243	58
					Validation Cohort					
1 Cer(d18:1/22:1)	2.89	4.970×10^{-2}	2	95	14	1	—	—	—	—
2 Cer(d18:1/24:1(15Z))	79.52	2.845×10^{-1}	2	95	14	2	—	—	—	—
3 DHCer(d18:0/16:0)	1.24	4.769×10^{-1}	2	88	21	3	7.427×10^{-2}	2	90	19
4 Cer(d18:1/20:0)	8.44	9.436×10^{-2}	2	74	35	4	5.282×10^{-2}	2	87	22
5 Cer(d18:1/25:0)	13.10	8.057×10^{-2}	2	95	14	5	5.282×10^{-2}	2	87	22
6 Cer(d18:1/16:0)	29.65	9.248×10^{-1}	2	58	51	6	5.282×10^{-2}	2	87	22
7 Cer(d18:1/18:0)	11.85	3.317×10^{-1}	2	69	40	7	5.282×10^{-2}	2	87	22
8 Cer(d18:1/26:0)	1.71	8.397×10^{-2}	2	88	21	8	3.875×10^{-2}	2	83	26
9 Cer(d18:1/22:0)	26.73	7.593×10^{-1}	2	27	82	9	3.875×10^{-2}	2	83	26
10 Cer(d18:1/24:0)	176.94	4.810×10^{-1}	2	97	12	10	3.875×10^{-2}	2	83	26
11 Cer(d18:1/14:0)	0.83	6.939×10^{-1}	1	30	79	11	3.437×10^{-2}	2	88	21
12 Cer(d18:1/23:0)	49.16	5.578×10^{-2}	2	96	13	12	3.875×10^{-2}	2	83	26

p < 0.05 was considered statistically significant. *Design: 1 = protective effect; 2 = harmful effect. †Number of ceramides in the signature.

1D-DDg = 1-dimensional data-driven grouping; SWVg = statistically-weighted voting grouping; other abbreviations as in Table 2.
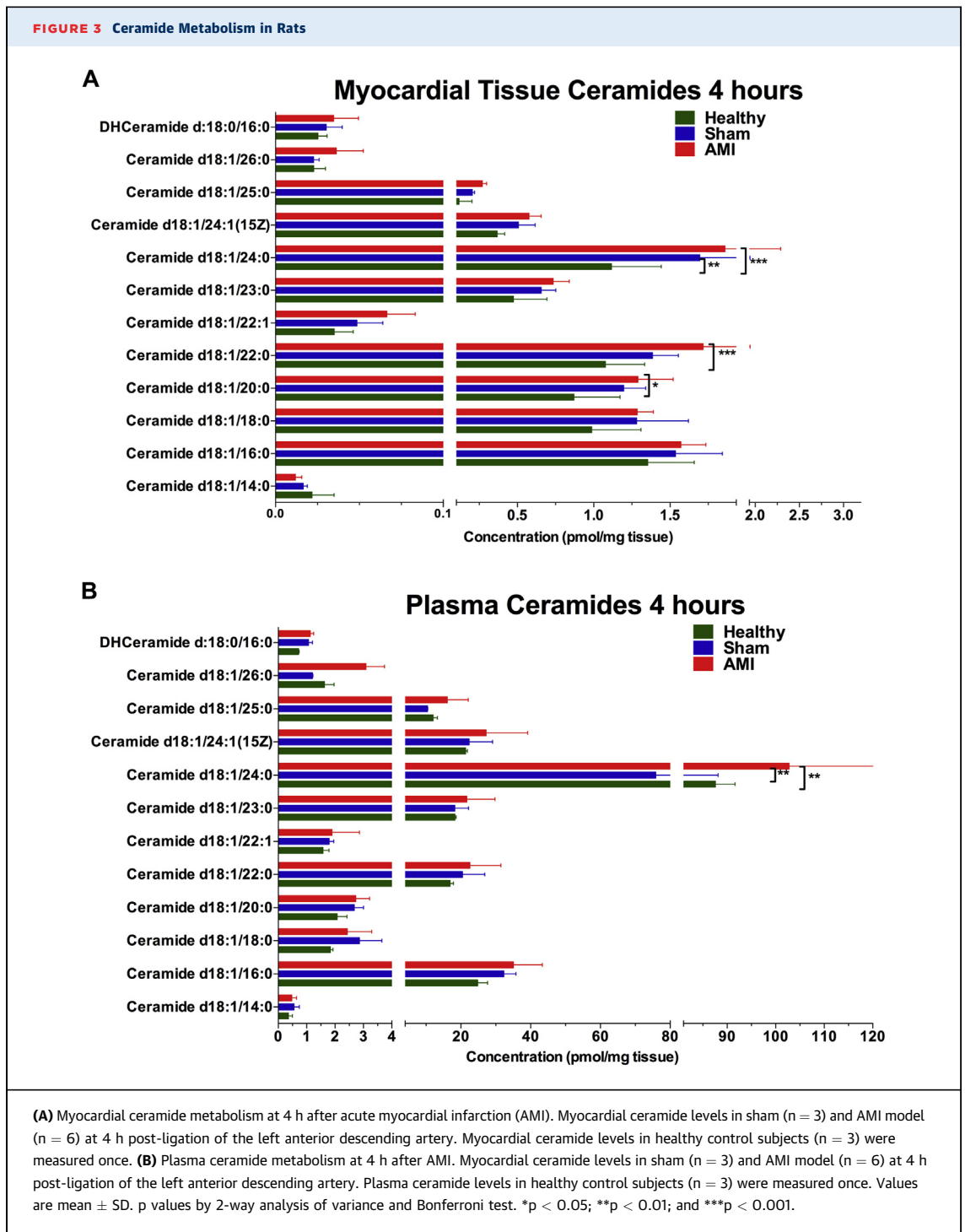
coronary artery occlusion. Although paired plasma samples from the same rat AMI model showed a numerical increase in the concentrations of all 12 ceramides, only the increase in plasma Cer(d18:1/24:0) was statistically significant when compared with sham and healthy control subjects.

CERAMIDES AND ATHEROSCLEROSIS. Atherosclerosis involves the ceramide pathway not only through ceramide-induced macrophage/foam cell apoptosis, but also via interactions with reactive oxygen species, nitric oxide, and inflammatory cytokines (23). In our study, the aortic tissue levels of ceramide species tended, albeit not significantly, to be higher in patients with versus without recent AMI undergoing bypass surgery. As confirmed in Supplemental Table 4, all patients in the bypass cohort had severe multivessel CAD. Aortic biopsies were obtained as remotely as 2 weeks after AMI, and more time-sensitive kinetic profiles might reveal greater enzyme turnover. The presence of a higher concentration of ceramides in plasma from the same patients with versus those without recent AMI suggests that sources other than arterial tissue, such as post-infarct myocardium, may be a continuing source of plasma ceramides 2 weeks after AMI.

CERAMIDES AND ISCHEMIC MYOCARDIAL INJURY. Mitochondrial dysfunction is a key event mediating cell death in ischemia-reperfusion injury, the insult leading to the many long-term sequelae in AMI, and ceramides are strongly implicated in mitochondrial-induced apoptotic cell death (6,27). Endogenous ceramides, generated from either de novo synthesis or sphingomyelinase activation in response to diverse cellular stress stimuli such as hypoxia, ischemia-reperfusion, chemotherapy, or γ-irradiation, mediate mitochondrial cytochrome C release and apoptosis of cardiomyocytes (27). Consistent with the pattern of increased ceramide production in our rat model of AMI, other studies have shown an increase in myocardial ceramide levels during ischemic-reperfusion injury with corresponding down-regulation of ceramidase activity (28,29) and

FIGURE 3   Ceramide Metabolism in Rats

(A) Myocardial ceramide metabolism at 4 h after acute myocardial infarction (AMI). Myocardial ceramide levels in sham (n = 3) and AMI model (n = 6) at 4 h post-ligation of the left anterior descending artery. Myocardial ceramide levels in healthy control subjects (n = 3) were measured once. **(B)** Plasma ceramide metabolism at 4 h after AMI. Myocardial ceramide levels in sham (n = 3) and AMI model (n = 6) at 4 h post-ligation of the left anterior descending artery. Plasma ceramide levels in healthy control subjects (n = 3) were measured once. Values are mean ± SD. p values by 2-way analysis of variance and Bonferroni test. *p < 0.05; **p < 0.01; and ***p < 0.001.

dramatic reciprocal up-regulation of SPT (30) and sphingomyelinase (31). Serine palmitoyl transferase is a key rate-limiting enzyme catalyzing the first step in the de novo synthesis of ceramides (32). Interestingly, the inhibition of SPT with myriocin protects cardiomyocytes from lipotoxic injury, suggesting a potential role for therapeutic ablation of the de novo

ceramide pathway to minimize myocardial injury (33). SMases hydrolyses sphingomyelin, releasing phospholcholines and ceramides. Ischemia-reperfusion leads to an elevation of SMase activities and subsequent activation of TNF-α mediated apoptosis (34). Meanwhile, the blockade of SMase activity with N-acetylcysteine abrogates TNF-α–induced apoptosis

and improves post-infarct cardiac recovery (35). Taken together, the inhibition of SPT and SMases could potentially ameliorate myocardial ischemia-reperfusion injury, attenuate apoptosis, and facilitate cardiac recovery.

Ceramide synthases regulate the synthesis of ceramides in both the de novo and salvage ceramide pathways. There are 6 known ceramide synthases, and each has a unique specificity for acyl CoA chain length (36). We observed an increase in rat myocardial CerS6 during AMI, which has been shown to generate mainly shorter-chain ceramides such as C14:0 and C16:0 (37). In agreement with our human data, rat myocardial Cer(d18:1/14:0) and Cer(d18:1/16:0) increased significantly 24 h after AMI.

ODD-CHAIN CERAMIDES AND DIHYDROCERAMIDES. We observed the presence of 2 odd-chain ceramides, Cer(d18:1/23:0) and Cer(d18:1/25:0), in the prognostic multiceramide signature. Odd-chain ceramides are derived from odd-chain saturated fatty acids, which are not endogenously produced in the human body. Dairy products and meat from ruminant animals are important sources of odd-chain saturated fatty acids (38). Population-based studies have found an inverse association between plasma odd-chain saturated fatty acids and the risk of coronary heart disease (39) and type 2 diabetes (40). Given the low abundance of the 2 odd-chain ceramides in both cohorts, we cannot exclude the possibility that they may represent an epiphenomenon rather than having a more direct role in AMI outcomes.

DHCer, which are transiently produced during de novo ceramide synthesis, have been deemed to be biologically inert (41). Recent evidence suggests that DHCer have biological functions that are distinct and nonoverlapping with those of the more prevalent ceramides, including autophagy, hypoxia, and cellular proliferation (41). Our prognostic ceramide signature only consists of 1 dihydroceramide, DHCer(18:0/16:0), but further research may better define the prognostic role of elevated plasma DHCer for secondary ischemic events.

STUDY LIMITATIONS. First, our discovery and validation cohorts were relatively small compared with other studies. Second, the highly dimensional nature of our datasets (larger number of predictors than events) necessitated the use of deep learning models (DDg and SWVg) to derive predictive signatures. Although this approach is able to delineate a ceramide signature that classifies patients into low versus high risk, our sample size does not permit the development of a quantitative risk score to predict the incidence of MACCE. Third, our study lacked other reference prognostic biomarkers such as B-type

natriuretic peptide and C-reactive protein. Fourth, the activation of lipoprotein lipase by heparin will continue to be a concern for all lipidomic studies. Lipoprotein lipase catalyzes the breakdown of triglycerides in lipoproteins, which may affect the plasma lipidome (42). The intensities of ceramides measured on day 2 were also less than those on day 1, likely because heparin was stopped immediately after coronary angiography with or without percutaneous coronary intervention in patients with AMI. Indeed, this should be strongly considered when measuring plasma ceramides in clinical samples; testing for plasma ceramides as prognostic biomarkers is now being offered as a clinical test for patients with CAD (43), and patients with CAD are often exposed to heparin in the inpatient setting. Fifth, our paired analysis of arterial tissue and plasma in patients with and without AMI utilized punch biopsies of the thoracic aorta instead of coronary artery segments. Although access to coronary artery tissue remains a limitation of many human studies similar to ours, numerous studies have established a strong correlation between atherosclerotic disease severity of the thoracic aorta and coronary arteries (44-46).

A key strength of our study is the verification of the presence of the 12-ceramide prognostic signature in paired aortic tissue-plasma and paired myocardial tissue-plasma samples. To our knowledge, no prior published studies have simultaneously profiled a singular ceramide signature in AMI cohorts with longitudinal outcomes, paired aortic tissue-plasma samples, and paired myocardial tissue-plasma samples.

CONCLUSIONS

A 12-ceramide plasma prognostic signature comprising 9 even-chain ceramides, 2 odd-chain ceramides, and 1 dihydroceramide of C14-26 chain length was associated with cardiovascular death, recurrent MI, and stroke after an AMI in ethnically diverse cohorts. Taken together with other studies, our data support a prognostic role of plasma ceramide species in AMI. The profiling of proposed multiceramide signature in arterial and myocardial tissue in recent and acute infarction, respectively, indicates an up-regulation of ceramide pathway enzymes in ischemic myocardium, which may be a source of plasma ceramides in AMI. Future studies are needed to clarify the role of odd-chain ceramides and dihydroceramide in mediating ischemic outcomes after AMI. The prognostic role of other complex ceramides such as glucosylceramides and lactosylceramides also deserves further study; such efforts will require a combination of quantitative lipidomic and glycomic platforms.

ADDRESS FOR CORRESPONDENCE: Dr. Mark Y. Chan, Cardiac Department, Yong Loo-Lin School of Medicine, National University of Singapore, 1E, Kent Ridge Road, NUHS Tower Block, Level 9, Singapore 119228. E-mail: mark_chan@nuhs.edu.sg. OR Dr. Vladimir A. Kuznetsov, Department of Urology, Department of Biochemistry and Molecular Biology, 750 East Adams Street, Weiskotten Hall, Room 1271, SUNY Upstate Medical University, Syracuse, New York 13210. E-mail: kuznetsv@upstate.edu.

PERSPECTIVES

COMPETENCY IN MEDICAL KNOWLEDGE: Plasma ceramides predict cardiovascular death, recurrent MI, and stroke after an AMI. Taken together with other studies, our data support a prognostic role of plasma ceramide species in AMI. The optimal time at which to perform testing appears to be 24 to 72 h after symptom onset.

TRANSLATIONAL OUTLOOK: Future studies are needed to clarify the role of odd-chain ceramides and dihydroceramide in mediating ischemic outcomes after AMI. The prognostic role of other complex ceramides such as glucosylceramides and lactosylceramides also deserves further study; such efforts will require a combination of quantitative lipidomic and glycomic platforms.

REFERENCES

1. Chaudhry SI, Khan RF, Chen J, et al. National trends in recurrent AMI hospitalizations 1 year after acute myocardial infarction in Medicare beneficiaries: 1999-2010. J Am Heart Assoc 2014;3:e001197.

2. Chatterjee S. Sphingolipids in atherosclerosis and vascular biology. Arterioscler Thromb Vasc Biol 1998:1523–33.

3. Mukhin DN, Chao FF, Kruth HS. Glycosphingolipid accumulation in the aortic wall is another feature of human atherosclerosis. Arterioscler Thromb Vasc Biol 1995;15:1607–15.

4. Wang DD, Toledo E, Hruby A, et al. Plasma ceramides, Mediterranean diet, and incident cardiovascular disease in the PREDIMED trial (Prevencion con Dieta Mediterranea). Circulation 2017; 135:2028–40.

5. Ogretmen B, Hannun YA. Biologically active sphingolipids in cancer pathogenesis and treatment. Nat Rev Cancer 2004;4:604–16.

6. Novgorodov SA, Gudz TI. Ceramide and mitochondria in ischemia/reperfusion. J Cardiovasc Pharmacol 2009;53:198–208.

7. Bielawska AE, Shapiro JP, Jiang L, et al. Ceramide is involved in triggering of cardiomyocyte apoptosis induced by ischemia and reperfusion. Am J Pathol 1997;151:1257–63.

8. Laaksonen R, Ekroos K, Sysi-Aho M, et al. Plasma ceramides predict cardiovascular death in patients with stable coronary artery disease and acute coronary syndromes beyond LDL-cholesterol. Eur Heart J 2016;37:1967–76.

9. Sigruener A, Kleber ME, Heimerl S, Liebisch G, Schmitz G, Maerz W. Glycerophospholipid and sphingolipid species and mortality: the Ludwigshafen Risk and Cardiovascular Health (LURIC) Study. PLOS ONE 2014;9:e85724.

10. Havulinna AS, Sysi-Aho M, Hilvo M, et al. Circulating ceramides predict cardiovascular outcomes in the population-based FINRISK 2002 cohort. Arterioscler Thromb Vasc Biol 2016;36:2424–30.

11. Thygesen K, Alpert JS, Jaffe AS, et al. Third universal definition of myocardial infarction. J Am Coll Cardiol 2012;60:1581–98.

12. Montalescot G, Sechtem U, Achenbach S, et al. 2013 ESC guidelines on the management of stable coronary artery disease. Eur Heart J 2013;34: 2949.

13. Overmyer KA, Thonusin C, Qi NR, Burant CF, Evans CR. Impact of anesthesia and euthanasia on metabolomics of mammalian tissues: studies in a C57BL/6J mouse model. PLoS One 2015;10: e0117232.

14. Chan MY, Shah BR, Gao F, et al. Recalibration of the Global Registry of Acute Coronary Events risk score in a multiethnic Asian population. Am Heart J 2011;162:291–9.

15. Grinchuk OV, Motakis E, Yenamandra SP, et al. Sense-antisense gene-pairs in breast cancer and associated pathological pathways. Oncotarget 2015;6:42197–221.

16. Tang Z, Ow GS, Thiery JP, Ivshina AV, Kuznetsov VA. Meta-analysis of transcriptome reveals let-7b as an unfavorable prognostic biomarker and predicts molecular and clinical subclasses in high-grade serous ovarian carcinoma. Int J Cancer 2014;134:306–18.

17. Chen L, Jenjaroenpun P, Pillai AM, et al. Transposon insertional mutagenesis in mice identifies human breast cancer susceptibility genes and signatures for stratification. Proc Natl Acad Sci U S A 2017;114:E2215–24.

18. Kuznetsov VA, Tang Z, Ivshina AV. Identification of common oncogenic and early developmental pathways in the ovarian carcinomas controlling by distinct prognostically significant microRNA subsets. BMC Genomics 2017; 18:692.

19. Ow GS, Kuznetsov VA. Big genomics and clinical data analytics strategies for precision cancer prognosis. Sci Rep 2016;6:36493.

20. Ow GS, Tang Z, Kuznetsov VA. Big data and computational biology strategy for personalized prognosis. Oncotarget 2016;7:40200–20.

21. ComBat. Available at: https://www.bu.edu/jlab/wp-assets/ComBat/Abstract.html. Accessed January 12, 2018.

22. SurvExpress. Available at: http://bioinformatica.mty.itesm.mx:8080/Biomatec/SurvivaX.jsp. Accessed January 12, 2018.

23. Bismuth J, Lin P, Yao Q, Chen C. Ceramide: a common pathway for atherosclerosis? Atherosclerosis 2008;196:497–504.

24. Hornemann T, Worgall TS. Sphingolipids and atherosclerosis. Atherosclerosis 2013;226: 16–28.

25. Edsfeldt A, Duner P, Stahlman M, et al. Sphingolipids contribute to human atherosclerotic plaque inflammation. Arterioscler Thromb Vasc Biol 2016;36:1132–40.

26. Jin J, Hou Q, Mullen TD, et al. Ceramide generated by sphingomyelin hydrolysis and the salvage pathway is involved in hypoxia/reoxygenation-induced Bax redistribution to mitochondria in NT-2 cells. J Biol Chem 2008;283: 26509–17.

27. Parra V, Moraga F, Kuzmicic J, et al. Calcium and mitochondrial metabolism in ceramide-induced cardiomyocyte death. Biochim Biophys Acta 2013;1832:1334–44.

28. Beresewicz A, Dobrzyn A, Gorski J. Accumulation of specific ceramides in ischemic/reperfused rat heart; effect of ischemic preconditioning. J Physiol Pharmacol 2002;53:371–82.

29. Zhang DX, Fryer RM, Hsu AK, et al. Production and metabolism of ceramide in normal and ischemic-reperfused myocardium of rats. Basic Res Cardiol 2001;96:267–74.

30. Reforgiato MR, Milano G, Fabrias G, et al. Inhibition of ceramide de novo synthesis as a postischemic strategy to reduce myocardial reperfusion injury. Basic Res Cardiol 2016;111:12.

31. Cordis GA, Yoshida T, Das DK. HPTLC analysis of sphingomyelin, ceramide and sphingosine in ischemic/reperfused rat heart. J Pharm Biomed Anal 1998;16:1189–93.

32. Hanada K. Serine palmitoyltransferase, a key enzyme of sphingolipid metabolism. Biochim Biophys Acta 2003;1632:16–30.

33. Park T-S, Hu Y, Noh H-L, et al. Ceramide is a cardiotoxin in lipotoxic cardiomyopathy. J Lipid Res 2008;49:2101–12.

34. Krown KA, Page MT, Nguyen C, et al. Tumor necrosis factor alpha-induced apoptosis in cardiac myocytes. Involvement of the sphingolipid signaling cascade in cardiac cell death. J Clin Invest 1996;98:2854–65.

35. Adamy C, Mulder P, Khouzami L, et al. Neutral sphingomyelinase inhibition participates to the benefits of acetylcysteine treatment in post-myocardial infarction failing heart rats. J Mol Cell Cardiol 2007;43:344–53.

36. Levy M, Futerman AH. Mammalian ceramide synthases. IUBMB life 2010;62:347–56.

37. Mizutani Y, Kihara A, Igarashi Y. Mammalian Lass6 and its related family members regulate synthesis of specific ceramides. Biochem J 2005; 390:263–71.

38. Jenkins B, West J, Koulman A. A review of odd-chain fatty acid metabolism and the role of pentadecanoic acid (C15:0) and heptadecanoic acid (C17:0) in health and disease. Molecules 2015; 20:2425.

39. Khaw K-T, Friesen MD, Riboli E, Luben R, Wareham N. Plasma phospholipid fatty acid concentration and incident coronary heart disease in men and women: the EPIC-Norfolk prospective study. PLoS Med 2012;9:e1001255.

40. Forouhi NG, Koulman A, Sharp SJ, et al. Differences in the prospective association between individual plasma phospholipid saturated fatty acids and incident type 2 diabetes: the EPIC-InterAct case-cohort study. Lancet Diabetes Endocrinol 2014;2:810–8.

41. Siddique MM, Li Y, Chaurasia B, Kaddai VA, Summers SA. Dihydroceramides: from bit players to lead actors. J Biol Chem 2015;290: 15371–9.

42. Brunner MP, Shah SH, Craig DM, et al. Effect of heparin administration on metabolomic profiles in samples obtained during cardiac catheterization. Circ Cardiovasc Genet 2011;4:695–700.

43. Mayo Clinic Laboratories. Test ID: CERAM. Ceramides, Plasma. Available at: http://www.

mayomedicallaboratories.com/test-catalog/Clinical+and+Interpretive/65054. Accessed August 15, 2017.

44. Fazio GP, Redberg RF, Winslow T, Schiller NB. Transesophageal echocardiographically detected atherosclerotic aortic plaque is a marker for coronary artery disease. J Am Coll Cardiol 1993;21:144–50.

45. Acarturk E, Demir M, Kanadasi M. Aortic atherosclerosis is a marker for significant coronary artery disease. Jpn Heart J 1999;40:775–81.

46. Gu X, He Y, Li Z, et al. Relation between the incidence, location, and extent of thoracic aortic atherosclerosis detected by transesophageal echocardiography and the extent of coronary artery disease by angiography. Am J Cardiol 2011; 107:175–8.

KEY WORDS acute coronary syndrome, ceramides, dihydroceramides, major adverse cardiovascular and cerebrovascular events, prognosis, risk prediction

APPENDIX For an expanded Methods section as well as supplemental figures and tables, please see the online version of this paper.

CME MOC ABIM ACCREDITED

Go to http://www.acc.org/jacc-journals-cme to take the CME/MOC quiz for this article.